Theory of the locomotion of nematodes

Dynamics of undulatory progression on a surface

Ernst Niebur and Paul Erdös
Institute of Theoretical Physics, University of Lausanne, CH-1015 Lausanne, Switzerland

ABSTRACT We develop a model of the undulatory locomotion of nematodes, in particular that of *Caenorhabditis elegans*, based on mechanics. The model takes into account the most important forces acting on a moving worm and allows the computer simulation of a creeping nematode. These forces are produced by the interior pressure in the liquid-filled body cavity, the elasticity of the cuticle, the excitation of certain sets of muscles and the friction between the body and its support.

We propose that muscle excitation patterns can be generated by stretch receptor control. By solving numerically the equations of motion of the model of the nematode, we demonstrate that these muscle excitation patterns are suitable for the propulsion of the animal.

INTRODUCTION

We present here a theoretical study of the control and mechanism of undulatory motion of nematodes (round worms) on a solid surface. In particular, we study the mechanical forces which are related to undulatory locomotion. In a related work, we have studied the propagation of neural signals and the control of the somatic motor neurons in nematodes (see Niebur and Erdös, 1991, and the Appendix of this paper). The output of the motor nervous system consists of patterns of muscle excitation which are suitable for generating the wavelike body shape and for propelling the body in a given direction. Because of Gray's pioneering work (Gray, 1953), we know that for creeping motion on a solid surface, it is necessary that the radius of curvature of the body vary along the body: only in this case can muscular forces produce a forward thrust. A simple explanation of this fact may be found in (Erdös and Niebur, 1990). The mechanics of undulatory locomotion is an interesting biological problem in itself. This mode of locomotion is used in a great variety of environments by thousands of animal species, varying in size from protozoa to snakes. Undulatory locomotion is also important in other fields, e.g., in robotics. There are environments which are not easily accessible (e.g., the interior of complex tube systems) and where a vermiform robot can move by undulatory propulsion (Niebur and Erdös, 1991).

In the next section, we present the locomotive apparatus of *Caenorhabditis elegans* (*C. elegans*). In sections following we present our model of the nematode body, a description of the mechanical forces evoked by a nematode when it is creeping over a solid surface and a description of the trajectory control. We then establish the equations of motion of the body and present an implementation of the model on a computer which allows us to simulate the locomotion of nematodes. Finally, the results of the computer simulation are shown and discussed and we present the conclusions.

Dr. Niebur's current address is Computation and Neural Systems Program, Division of Biology 216-76, California Institute of Technology, Pasadena, California 91125.

LOCOMOTIVE APPARATUS OF *C. ELEGANS*

Environment

The natural habitat of *C. elegans* consists of the interstices between the particles of the soil, which are covered by a water film. *C. elegans* lives in this water film. In the laboratory, *C. elegans* are usually kept in Petri dishes on an agar layer (see Brenner, 1974 for details). Although the worms are able to penetrate into the agar gel, they usually stay on the surface.

The surface is covered with a water film whose thickness depends on the concentration of the agar. If the thickness of the water film is less than the body diameter of a nematode, a surface tension results which presses the worm against the agar surface. A groove is produced, which partially encloses the body of the worm and enables it to exert lateral forces (perpendicular to the body surface) against the walls of the groove (Wallace, 1969). If the groove is sufficiently profound, no lateral movement of the worm's body is possible and each part of the worm is obliged to follow the immedi-

0006-3495/91/11/1132/15 $2.00

ately adjacent part of the body. We call this movement "creeping."

On more humid agar, the water film is thicker and the surface tension which presses the worm into the agar is weaker. As a result, the groove is shallower and the lateral forces are able to cause lateral movements, consequently the worm "slips." If the thickness of the water film exceeds the body diameter, the worm is totally immersed in the water and its swims.

Consider the forward movement of a nematode in the three environments, which lead to creeping, creeping with slipping, and swimming. Because *C. elegans* is normally lying on its side, the concepts dorsal/ventral are equivalent to left/right. *C. elegans* moves actively by throwing its body in dorso-ventral bends, which give the worm a sinusoidal shape. When creeping, the head of the worm pursues a sinusoidal curve and all other parts of its body follow. The waves, called "muscular waves," which are formed by the body, are stationary with respect to the support. They travel with the same velocity backwards in the reference frame of the worm as the worm travels forwards in the reference frame of the support. When the worm moves with lateral slipping, the absolute value of the velocity of the muscular waves is greater than the speed of the worm. When the worm swims, it is observed that the velocity of the muscular waves is much greater than that of the worm (Gray and Lissmann, 1964).

Hydrostatic skeleton

The body of an adult *C. elegans* has approximately the shape of a cylinder with a diameter of ~ 80 μm and length 1 mm. It is ensheathed by an elastic cuticle whose inner surface is covered by a muscle layer, which will be described in more detail below. This layer encloses the "pseudo-coelom," a nonsegmented cavity which contains the intestine, the gonads, and liquid. The liquid is under considerable pressure with respect to the exterior. In the larger nematode *Ascaris lumbricoides*, the pressure can be measured experimentally. A typical value is 10^4 Pa, and in extreme cases, $3 \cdot 10^4$ Pa (Lee and Atkinson, 1976).

In the nematodes, the body muscles deform the elastic cuticle by exerting their contractive force against the interior pressure. When the muscles relax, the interior pressure restores the original length of the muscles. Following Harris and Crofton, (1957), we will call this structure the "hydrostatic skeleton."

Inextensible fibers in the nematode cuticle

The cuticles of adult large *Ascarids* contain fibers which are practically inextensible and which spiral in three layers geodetically around the body. It is tempting to assume that the mechanical properties of the cuticle are determined by these fibers, because this would yield a solid base for a quantitative theory of the cuticle deformations. It was believed that the inextensible fibers are present in the cuticles of all nematodes (Harris and Crofton, 1957). Later, their presence in the cuticles of small nonparasitic species was doubted (Bird, 1971). More recently, fibers were found in adult *C. elegans*, which is a small, nonparasitic nematode, but not in Dauerlarvae of *C. elegans* (Edgar et al., 1982). These larvae move, however, in the same way as the adults do. Other workers (Thust, 1966; Morseth and Soulsby, 1969; Fredericksen and Specian, 1981) have shown that fibers are present in the cuticles of second and third stage larvae of *Ascaris l.*, but that the fibers are arranged randomly and not in layers of geodetical spirals.

To summarize, there are several examples where either no inextensible fibers are found in the cuticle of nematodes or where these fibers are not arranged in structured layers. In all these cases, the animals move by undulatory locomotion. We conclude that a theoretical explanation of this locomotion cannot be based on the existence of inextensible fibers in the cuticle. In the section on computer simulation, we will present a realistic physical model of the nematode body.

Musculature used for locomotion

It was noted above that the interior of the cuticle is covered by a layer of muscle cells which are used for the locomotion. The contractile parts of all these muscle cells (95 in *C. elegans*, $\sim$ 50,000 in *Ascaris l.*) are parallel to the long axis of the worm; there are no circular muscles. The musculature is divided in two half-cylinders, one of which is innervated by the dorsal motor neurons and the other one by the ventral motor neurons. There is no finer subdivision of the innervation. This structure explains the observation that the body of nematodes moves by dorso-ventral bends. The muscles of the head receive a more detailed and more complicated innervation (White et al., 1986), which permits it to move outside the dorso-ventral plane.

In nematodes, the muscle cells send out processes to the neural process tracts, where they interdigitate extensively and make neuromuscular junctions (NMJs) with the neurons. In the proximity of the NMJs, the muscle cell processes are coupled electrically, and graded action potentials are produced in this region, which are correlated with muscle contractions (Weisblat and Russell, 1976). For this reason, it has been proposed that the muscle activity is under myogenic control (Crofton, 1971).

This hypothesis is not necessary. In fact, it has been suggested that the electrical coupling between muscle processes could compensate for differences of excitation between adjacent cells that are too vast to allow smooth locomotion (Weisblat and Russell, 1976), or that the coupling compensates for irregularities in the innervation of neighboring muscle arms (Stretton, 1976).

Also, the action potentials generated in the muscle cells are necessary if the muscles are controlled by the neurons. It is not possible to transmit an appreciable voltage change from the NMJs to the muscle cells via the thin muscle cell processes by means of electrotonic voltage spread alone. The reason for this is the impedance mismatch between the high-ohmic muscle cell processes and the low-ohmic soma and contractile parts of the cell.

For these reasons, and in agreement with other authors (e.g., Johnson and Stretton, 1980), we make the hypothesis that it is the neural system of the worm which controls the locomotion. The muscle cells will be considered as simple mechanical elements, which contract when they are excited by the neurons.

Swimming of small nematodes

Theories exist which explain the swimming of fish or flagella (see, e.g., Nachtigall, 1983; Brokaw, 1985; Rikmenspoel, 1978); however, it is not possible to use these theories for analyzing the swimming of small nematodes like *C. elegans.*

The character of the forces which act on a body that is immersed in a liquid is determined by the Reynolds number N_R, which represents the ratio between the inertial forces and the viscous forces acting on the immersed body. N_R is defined by

$$N_R = Lv\rho/\mu,$$

where the symbols have the following meaning: L: one of the physical dimensions of the immersed body; v: relative velocity between the liquid and the immersed body; ρ: density of the liquid; μ: viscosity of the liquid.

Table 1 shows v, L, and N_R (calculated by us) for a flagellum, a fish considered typical, and for *C. elegans,* all swimming in water. For a swimming fish, the viscous forces can be neglected, and for the flagellum, the inertial forces can be neglected. For a small nematode like *C. elegans,* N_R is of order unity, and neither the viscous nor the inertial forces can be neglected. The analysis of the swimming of small nematodes is thus more complicated than it is for fish or flagella. For this reason, we will concentrate in this work on the creeping motion of nematodes on a solid surface.

Gray and Lissmann (1964) studied the behavior of a rubber cylinder which swims in water. According to their description of the cylinder, its Reynolds number must have been $>10^4$. These authors used the results of experiments with the rubber cylinder to draw conclusions about the swimming of small nematodes, whose body sizes and velocities are comparable to those shown for *C. elegans* in Table 1. A reduced or enlarged model of a physical system shows the same phenomena as the original only if their Reynolds numbers are equal. Because this condition is not fulfilled in the case of the rubber-cylinder model for small nematodes, the conclusions drawn by Gray and Lissman are questionable. To establish the hydrodynamic similarity in this case, one would have to place the rubber cylinder in a highly viscous liquid instead of water (Niebur, 1988).

TABLE 1 Reynolds number N_R of three organisms swimming in water

Organism	v [m/s]	L [m]	N_R
(*a*) Flagellum (*Chaetopterus*)	$1 \cdot 10^{-4}$	$31 \cdot 10^{-6}$	$3 \cdot 10^{-3}$
(*b*) *C. elegans*	$2 \cdot 10^{-3}$	10^{-3}	2
(*c*) Fish (typical)	10^{-1}	10^{-1}	10^4

v: velocity of locomotion; L: length of the body; (a) v and L from Brokaw (1985), Table 1; (b) (Niebur and Erdös, 1988*a*, *b*). Similar velocities have been observed for other nematodes of comparable size (Gray and Lissmann, 1964).

MODEL OF VERMIFORM BODIES WITH HYDROSTATIC SKELETONS

Aim of the model and assumptions

In this Section, we develop a mathematical model of the locomotion of a worm which has a hydrostatic skeleton such as *C. elegans.* Our model takes into account the forces which are exerted by (*a*) the pressure of the liquid in the pseudo-coelom of the worm, (*b*) the elastic forces of the cuticle, (*c*) the muscular forces, and (*d*) the frictional forces resulting from the interaction between the worm and its environment. It is explained in the previous section and in the next section why other forces can be neglected. We obtain the equation of motion in the form of a system of coupled first-order ordinary differential equations. The simulation of the motion of the nematode is achieved by solving this system of equations numerically on a computer.

Other assumptions will be discussed in detail whenever they are introduced. Here we list them for reference: (*a*) the liquid pressure is the same everywhere in the pseudo-coelom, and the total body volume is con-

served within specified limits (see, e.g., the next section, "Forces exerted by the environment"); (*b*) the elastic forces of the cuticle depend linearly on the length of the segment in which they act. A small elastic constant is chosen for small deviation from the equilibrium length, and a large constant is used if the deviation exceeds a certain limit, or if the cuticle is stretched perpendicularly to the local body axis; (*c*) the muscular forces act parallel to the local body axis; (*d*) the coefficient of the frictional forces is smaller for longitudinal than for transversal motion.

Further, it is assumed that either the head or the tail execute a periodic sideways motion which leads to a sinusoidal body shape.

Definition of the two-dimensional model

We approximate the body of the worm by a cylinder of length l_c and of radius r_c. (In fact, l_c and r_c refer to the state of the body with forces absent. The actual length and radius depend on the forces which act on the body wall and which will be introduced below.) Because we are interested in the movement in a plane, namely on the surface of the agar layer, we consider the projection of the cylinder on this plane. The outline of the projection is a closed curve which is shown in Fig. 1. For the simulation, N points are distributed on the left side of this curve and N points on its right side, so that the curve is divided in $(N - 1)$ segments. The term "segment" should not be understood in the sense that all the segments are identical or that their shape is fixed. Instead, all segments can change their size and their shape under the influence of the forces.

We denote all vectors with bold characters. The ith segment is described by the four points by which it is limited: $\mathbf{x}_r(i)$ and $\mathbf{x}_r(i + 1)$ on the right side of the body, and $\mathbf{x}_l(i)$ and $\mathbf{x}_l(i + 1)$ on the left side (see Fig. 1). Left and right are defined arbitrarily, but once and for all, we adopt the definition shown in Fig. 1. We use the subscripts r for right and l for left. The following equations are meant to be valid for all values of the index i for which the equation makes sense, i.e., either $i \in \{1, \ldots, N\}$ or $i \in \{1, \ldots, N - 1\}$, unless noted otherwise.

Let us define

$$x_i = i \frac{l_c}{N}, \tag{1}$$

$$u_i = A \cos(kx_i), \tag{2}$$

where k is the wave number and A the amplitude of the sinusoidal wave which is formed by the body of the worm ($k > 0, A > 0$).

We suppose that at $t = 0$, the coordinates of the points $\mathbf{x}_r(i)$ and $\mathbf{x}_l(i)$ are given by

$$\mathbf{x}_s(i) = \begin{pmatrix} x_s(i) \\ y_s(i) \end{pmatrix}, \quad s = r, l \tag{3}$$

$$x_s(i) = l_i - \frac{u_i}{\sqrt{1 + u_i^2}}, \tag{4}$$

$$y_s(i) = A \sin(kl_i) + \frac{u_i}{\sqrt{1 + u_i^2}}. \tag{5}$$

It follows from Eqs. 3–5 that the midpoints of the body, defined by

$$\mathbf{x}_c(i) = \begin{pmatrix} x_c(i) \\ y_c(i) \end{pmatrix} = \tfrac{1}{2} [\mathbf{x}_l(i) + \mathbf{x}_r(i)], \tag{6}$$

are situated on a sine curve:

$$y_c(i) = A \sin [k x_c(i)] \tag{7}$$

Fig. 1 shows the shape of the body which is defined by Eqs. 3–5.

FORCES ACTING ON THE BODY

Interior pressure

Let $p(t)$ be the pressure of the liquid which is contained in the body cavity of the worm (in nematodes, the pseudo-coelom). We assume that the cavity is not subdivided, which is the case for nematodes. It follows that the pressure is the same in all segments. The pressure at the borderline between two segments has no effect, because the forces involved are equal and opposite. For this reason, we have to take into account only pressures which act on the body wall. In our model, the body wall is represented by the two lateral limits of each segment, except in the case of the final segments ($i = 1$ and $i = N - 1$), which have three limits in contact with the exterior. We approximate each segment by a block, which lies on the plane of locomotion and whose height is $2r_c$.

The pressure is time dependent, because the volume of the liquid, which we assume to be incompressible, is constant. Numerically, we have enforced the constant-volume constraint as follows: we define the vectors $\mathbf{d}(i)$ and $\mathbf{e}(i)$, which are directed along the diagonals of segment i, by,

$$\mathbf{d}(i) = \mathbf{x}_r(i + 1) - \mathbf{x}_l(i), \tag{8}$$

$$\mathbf{e}(i) = \mathbf{x}_r(i) - \mathbf{x}_l(i + 1). \tag{9}$$

Let $p(0)$ and $V(0)$ be the pressure and volume of the worm, respectively, at time $t = 0$. We calculate the volume $V(t)$ from the shape of the body at time t, using

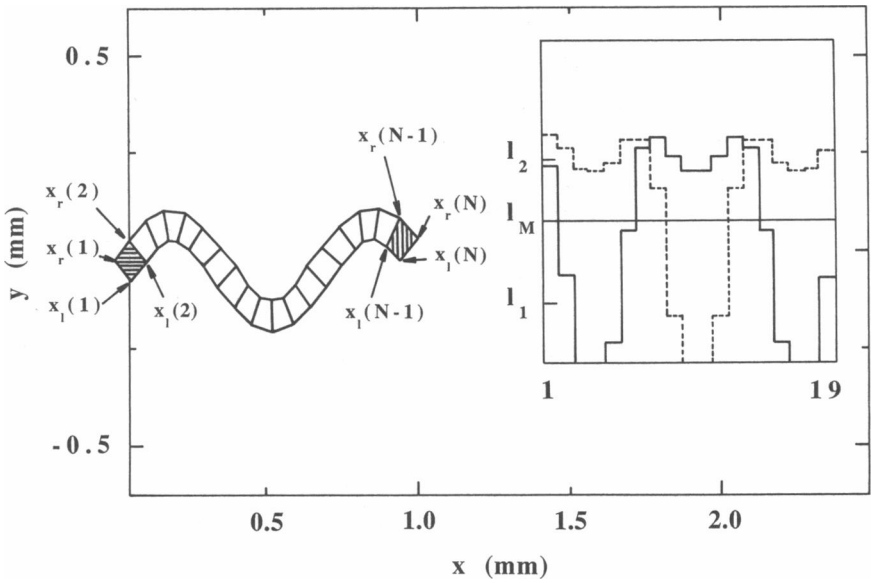

FIGURE 1 Two-dimensional model of the vermiform body, as defined by Eqs. 3–5 for $A = 3r_c$ and $k = 3\pi l_c^{-1}$. The parameters given in Table 2 are used. Each one of the points $\{x_r(i); x_l(i)$ for $i = 1, 2, \ldots, N\}$ is connected to its neighbors by a line. Segment 1, which is limited by the points $x_l(1)$, $x_l(2)$, $x_r(1)$, and $x_r(2)$ is shown with horizontal hatching. Segment $N - 1$ (i.e., segment 19), which is limited by the points $x_l(N-1)$, $x_l(N)$, $x_r(N-1)$, and $x_r(N)$ is shown with vertical hatching. In the inset, the length of each one of the 19 segments is plotted against the segment number. The full line represents the segment length on the left body side, i.e., $|x_l(i) - x_l(i+1)|$ vs. i, and the dotted line represents the segment length on the right body side, i. e., $|x_r(i) - x_r(i+1)|$ vs. i. The quantities l_1 and l_2, defined in Eq. 26 are indicated on the vertical axis. The mean length of all segments, l_M, is defined in Eq. 50 and is represented by a horizontal line.

the formula,

$$V(t) = 2r_c \sum_{i=1}^{N-1} |d^{(x)}(i)e^{(y)}(i) - d^{(y)}(i)e^{(x)}(i)|, \qquad (10)$$

where the superscripts refer to the corresponding components of the vectors.

The pressure at time t is then calculated from $V(t)$ by

$$p(t) = \left[\frac{p(0)V(0)}{V(t)}\right]^a, \qquad (11)$$

where a is a positive integer. (In this equation, p is dimensionless, i.e., divided by the unit of pressure.) We used $a = 4$, $a = 6$, or $a = 8$ with nearly identical results. For all these choices, we obtained, for the muscular forces used in the simulations, that

$$\left|\frac{V(t) - V(0)}{V(0)}\right| < 10^{-2} \quad \text{for all } t.$$

This shows that the volume remains reasonably constant. We will write p instead of $p(t)$ in the rest of this paper, to simplify the notation.

The interior pressure of some nematodes has been observed to change by more than a factor of 2. This has not been observed in *C. elegans.*, but if it were the case, a large value of a in Eq. 11 would allow for such pressure changes while keeping the volume nearly constant. The results with $a = 4$, 6, or 8 indicate that the conclusions of this paper will remain valid for higher a as well. Because the contents of the pseudo-coelom is no ideal liquid, volume changes are expected at very high pressure.

Because we consider vectors in a plane, for each such vector $\mathbf{X}$, we can define another vector $\mathbf{X}_\perp$ in this plane such that $\mathbf{X} \cdot \mathbf{X}_\perp = 0$ and $\mathbf{X}_\perp \cdot \mathbf{X}_\perp = \mathbf{X} \cdot \mathbf{X}$. The vector $\mathbf{X}_\perp$, which will be called "orthogonal to $\mathbf{X}$," is defined by the two equations in the last sentence, except for its sign. For the Eqs. 12, 14, and 16, this sign will be determined by the sign of the scalar products in the inequalities (13), (15), and (17), respectively.

Let us consider one of the interior segments. We introduce the term "pressure force," defined as the force exerted at the point $x_r(i)$ that is proportional to the interior pressure and to the surface area of the segment (see Fig. 2). It is directed perpendicularly to this surface:

$$\mathbf{F}_s^{(p)}(i) = pr_c[\mathbf{x}_s(i+1) - \mathbf{x}_s(i-1)]_\perp \quad s = r,l;$$
$$i \in \{2, \ldots, N-2\}, \qquad (12)$$

and it is directed outward from the body. This is the case if the sign of $\mathbf{F}_r^{(p)}(i)$ is determined by requiring,

$$\mathbf{F}_r^{(p)}(i) \cdot [\mathbf{x}_r(i) - \mathbf{x}_l(i)] > 0, \quad i \in \{1, \ldots, N-1\}. \qquad (13)$$

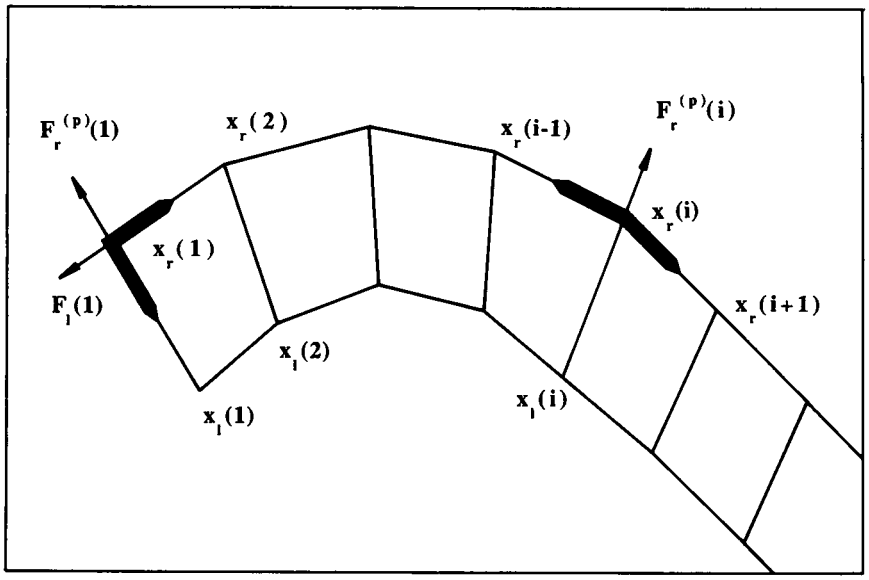

FIGURE 2 The interior pressure exerts forces on the body wall which are directed outwards. The figure shows a part of a vermiform body, whose body wall and the limits between segments are shown by thin lines. The pressure forces acting on two points, $x_r(5)$ and $x_r(1)$, are shown. The former is an interior point on which the force $F_r^{(p)}(5)$ acts, cf Eqs. 12 and 13. The latter is a boundary point, on which the forces $F_r^{(p)}(1)$ and $F_t(1)$ act, cf Eqs. 14, 15, and 18. The parts of the body wall on which these pressure forces act are represented in the figure by thick lines.

The force which acts on the point $\mathbf{x}_l(i)$ is obtained by the same expressions, after interchanging the subscripts r and l.

Let us now consider the pressure forces in the final segments (segments 1 and $N - 1$). One half of the force on the right lateral surface of segment 1 acts on $\mathbf{x}_r(2)$. This is taken into account in Eqs. 12 and 13. The other half of the force acts on $\mathbf{x}_r(1)$, and is given by

$$\mathbf{F}_r^{(p)}(1) = pr_c[\mathbf{x}_r(2) - \mathbf{x}_r(1)]_\perp, \tag{14}$$

where

$$\mathbf{F}_r^{(p)}(1) \cdot [\mathbf{x}_r(1) - \mathbf{x}_l(1)] > 0. \tag{15}$$

The pressure on the face of the cylinder (see Fig. 2) gives rise to another force, half of which acts on $\mathbf{x}_r(1)$ and the other half on $\mathbf{x}_l(1)$. The force acting on each of these points is $\mathbf{F}_t(1)$, calculated as

$$\mathbf{F}_t(1) = pr_c[\mathbf{x}_l(1) - \mathbf{x}_r(1)]_\perp, \tag{16}$$

where the sign of $\mathbf{F}_t(1)$ is determined by requiring

$$\mathbf{F}_t(1) \cdot [\mathbf{x}_r(1) - \mathbf{x}_r(2)] > 0. \tag{17}$$

The total pressure force which is exerted by the interior pressure on the point $\mathbf{x}_r(1)$ is thus

$$\mathbf{F}_r^{(p)}(1) + \mathbf{F}_t(1). \tag{18}$$

The pressure forces acting on $\mathbf{x}_l(1)$, $\mathbf{x}_r(N)$, and $\mathbf{x}_l(N)$ are obtained analogously.

Forces of the elastic cuticle

Our model of the cuticle consists of elastic elements between neighboring points of the cuticle. The neighbor points of $\mathbf{x}_r(i)$ are $\mathbf{x}_r(i - 1)$, $\mathbf{x}_r(i + 1)$ and $\mathbf{x}_l(i)$, and the neighbor points of $\mathbf{x}_l(i)$ are $\mathbf{x}_l(i - 1)$, $\mathbf{x}_l(i + 1)$, and $\mathbf{x}_r(i)$. We will first introduce the elastic forces between contralateral points [like $\mathbf{x}_r(i)$ and $\mathbf{x}_l(i)$] and then the forces between the ipsilateral points [like $\mathbf{x}_r(i)$ and $\mathbf{x}_r(i + 1)$].

It is observed experimentally that the body diameter of nematodes is practically constant in time. This is taken into account by assuming that the elastic element between $\mathbf{x}_r(i)$ and $\mathbf{x}_l(i)$ exerts the following force on $\mathbf{x}_r(i)$:

$$\mathbf{F}_r^{(e)}(i) = k_\perp \left[\frac{|\mathbf{x}_l(i) - \mathbf{x}_r(i)|}{2r_c} - 1\right][\mathbf{x}_l(i) - \mathbf{x}_r(i)], \tag{19}$$

where $k_\perp$ is a positive constant. The elastic element exerts the negative of this force on $\mathbf{x}_l(i)$:

$$\mathbf{F}_l^{(e)}(i) = -\mathbf{F}_r^{(e)}(i). \tag{20}$$

If the diameter of the segment is equal to $2r_c$, it follows from Eq. 19 that $\mathbf{F}_l^{(e)}(i) = \mathbf{F}_r^{(e)}(i) = 0$. If the diameter is different from $2r_c$, the forces will try to reestablish this equilibrium situation.

If $k_\perp$ is sufficiently great, the distance between $\mathbf{x}_l(i)$ and $\mathbf{x}_r(i)$ will differ only very little from $2r_c$. We have chosen

$$k_\perp = 10^3 \cdot k_l, \tag{21}$$

where k_l, which will be defined in Eq. 26, is an elastic constant of the forces between ipsilateral points.

We will treat now the ipsilateral forces. The segments can be easily deformed when their length is close to the equilibrium length l, but they resist strongly both excessive stretching and compression (see Fig. 3).

Consider the right side of the body. Let $\mathbf{F}_r^{(e)}(i, i+1)$ be the force (note that the contralateral forces have only one argument, e.g., $\mathbf{F}_r^{(c)}(i)$, and the ipsilateral forces have two arguments, e.g., $\mathbf{F}_r^{(e)}(i, i+1)$) which is exerted on the point $\mathbf{x}_r(i)$ by the elastic element between the points $\mathbf{x}_r(i)$ and $\mathbf{x}_r(i+1)$. It follows that this element exerts on the point $\mathbf{x}_r(i+1)$ the force

$$\mathbf{F}_r^{(e)}(i+1, i) = -\mathbf{F}_r^{(e)}(i, i+1). \tag{22}$$

The force $\mathbf{F}_r^{(e)}(i, i+1)$ is collinear to the vector $[\mathbf{x}_r(i+1) - \mathbf{x}_r(i)]$. It is defined by

$$\mathbf{F}_r^{(e)}(i, i+1) = f_r^{(e)}(i, i+1) \cdot \frac{1}{l_r(i)} \cdot [\mathbf{x}_r(i+1) - \mathbf{x}_r(i)], \tag{23}$$

where

$$l_r(i) = |x_r(i+1) - x_r(i)|, \tag{24}$$

$$f_r^{(e)}(i, i+1) = \begin{cases} k_3 \cdot [l_r(i) - l_2] + k_1 \cdot [l_2 - l_0] + \tfrac{1}{2}F_a & \text{if } l(i) > l_2 \\ k_2 \cdot [l_r(i) - l_1] + k_1 \cdot [l_1 - l_0] + \tfrac{1}{2}F_a & \text{if } l(i) < l_1 \\ k_1 \cdot [l_r(i) - l_0] + \tfrac{1}{2}F_a & \text{otherwise.} \end{cases} \tag{25}$$

The function $f_r^{(e)}(i, i+1)$ reproduces the characteristic behavior of the force shown in Fig. 3.

In the numerical work, we have used the following values:

$$\begin{aligned} k_1 &= \frac{F_a}{l_0}; \\ k_2 &= k_3 = 10k_1; \\ F_a &= 4p(0)r_c^2; \\ l_1 &= \frac{l_c}{N}; \\ l_0 &= \tfrac{5}{4}l_1; \\ l_2 &= \tfrac{3}{2}l_1. \end{aligned} \tag{26}$$

The elastic forces defined in Eq. 23 are in equilibrium with the pressure forces generated by an interior pressure $p(0)$ if all segments have the length l_0 and if $[\mathbf{x}_r(i) - \mathbf{x}_l(i)] = 2r_c$ for all i.

The forces of the left side are obtained analogously.

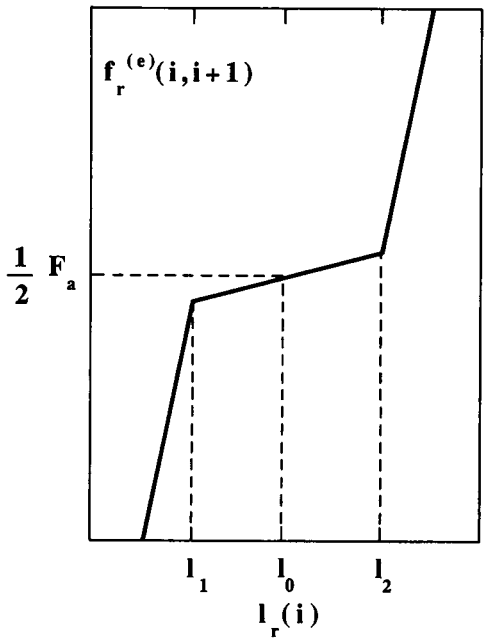

FIGURE 3 Elastic force assumed to act between two ipsilateral points, i.e., end points on the same side of a given segment, as a function of the distance between them. $f_r^{(e)}(i, i+1)$, defined in Eq. 25, is plotted as a function of $l_r(i)$, defined in Eq. 24. The ordinate is proportional to the force acting along the two endpoints of the segment; the abscissa is the distance between these points. The slope has the value k_2 for $l(i) < l_1$, k_1 for $l_1 < l(i) < l_2$, and k_3 for $l(i) > l_2$. This ensures that the force is small when the cuticle is only slightly stretched or compressed, but is large when the cuticle is overstretched or overcompressed.

Muscle forces

It was noted previously that the main (somatic) musculature of nematodes consists exclusively of longitudinal muscles. For this reason, we introduce model muscles which exert contracting forces between neighboring ipsilateral points. We consider the right side of the body; the results for the left side are obtained by replacing all subscripts r by l. Let $\mathbf{F}_r^{(m)}(i, i+1)$ be the force which is exerted at the point $\mathbf{x}_r(i)$ by the muscle acting between $\mathbf{x}_r(i)$ and $\mathbf{x}_r(i+1)$. The same muscle exerts the force,

$$\mathbf{F}_r^{(m)}(i+1, i) = -\mathbf{F}_r^{(m)}(i, i+1), \tag{27}$$

on the point $\mathbf{x}_r(i+1)$. The force $\mathbf{F}_r^{(m)}(i, i+1)$ is collinear to $\mathbf{x}_r(i+1) - \mathbf{x}_r(i)$, and it has the same direction. In our model, its absolute value is

$$|\mathbf{F}_r^{(m)}(i+1, i)| = f_r^{(m)}(i) \cdot k_1 \cdot l_0; \quad i \in \{2, \ldots, N-2\}. \tag{28}$$

Here, $f_r^{(m)}(i)$ is a dimensionless number which depends on the excitation status of the motor neurons which are presynaptic to the muscles in segment i. This number expresses the proportionality between the muscle force in segment i and the elastic force in a segment in equilibrium with the average (i.e., constant) pressure forces.

The set of numbers

$$\{f_l^{(m)}(i); f_r^{(m)}(i) \quad \text{for } i = 2; 3; \ldots; N-2\},$$

defines the "excitation pattern" of the muscles of the body in the sense that the number $f_s^{(m)}(i)$, $(s = r, l)$ is proportional to the momentary amplitude of the muscle force in the segment i. The muscular force is identically zero in the first and last segments ($i = 1$ and $i = N - 1$). In the section on computer simulation of undulatory locomotion, we will study those excitation patterns which lead to the undulatory locomotion of the worm.

According to Eq. 28, the muscular force does not depend on the length of the muscle. Indeed, the obliquely striated muscles of nematodes develop forces nearly independent of their length (Toida et al., 1975).

Forces exerted by the environment

The mass of a *C. elegans* is $\sim 5 \cdot 10^{-9}$ kg. The maximal acceleration produced during the creeping of this nematode on a solid surface is of the order of 10^{-3} m/s^2. It follows that the inertial forces during this movement are $\sim 5 \cdot 10^{-12}$ kg m/s^2.

The actual forces that a creeping nematode exerts on its support have not been measured. To determine these forces at least approximately, Wallace (1969) measured the friction forces needed to draw glass fibers of the same size as a small nematode over an agar surface. He found forces between $17 \cdot 10^{-6}$ kg m/s^2 and $72 \cdot 10^{-6}$ kg m/s^2, depending on the concentration of the agar.

To move, the worm has to exert forces on its environment which equal or exceed the frictional forces. Because these forces are by several orders of magnitude greater than the inertial forces, we will neglect the latter.

Let $\mathbf{x}_s(j)$, $s = r, l$ be the position of one of the $2N$ mass points, introduced in Eq. 1 and shown in Fig. 2. The ensemble of the vectors $\mathbf{x}_s(j)$ describes the position of the body at a given time t, but we do not write the variable t explicitely. The velocity of the point $\mathbf{x}_s(j)$ is $\mathbf{v}_s(j)$, i.e.,

$$\mathbf{v}_s(j) = \frac{d}{dt}\mathbf{x}_s(j), \quad s = r, l. \tag{29}$$

We can resolve $\mathbf{v}_s(j)$ in the components $\mathbf{v}_s^L(j)$ and $\mathbf{v}_s^N(j)$, which are longitudinal (L) and normal (N) with respect to the local body axis at the point $\mathbf{x}_s(j)$. By $\mathbf{t}(j)$ we denote a unit vector in the direction of the local body axis, i.e.,

$$\mathbf{t}(j) = \frac{\mathbf{x}_s(j+1) - \mathbf{x}_s(j-1)}{|\mathbf{x}_s(j+1) - \mathbf{x}_s(j-1)|}. \tag{30}$$

In a good approximation $\mathbf{t}(j)$ is independent of s, hence we omit this subscript. Then

$$\mathbf{v}^L(j) = [\mathbf{v}(j) \cdot \mathbf{t}(j)]\mathbf{t}(j), \quad j \in \{2, \ldots, N-1\}, \tag{31}$$

and

$$\mathbf{v}^N(j) = \mathbf{v}(j) - \mathbf{v}^L(j). \tag{32}$$

For the endpoints of the model worm we have

$$\mathbf{v}^L(1) = [\mathbf{v}(1) \cdot \mathbf{t}(1)]\mathbf{t}(1), \tag{33}$$

and

$$\mathbf{v}^L(N) = [\mathbf{v}(N) \cdot \mathbf{t}(N-1)]\mathbf{t}(N-1). \tag{34}$$

We formulate now our model of the exterior, frictional forces, which act between the worm and its environment. We assume that these $2N$ forces, acting on each of the points $x_s(j)$, are of the form

$$\mathbf{F}_s^f(j) = -c_L\mathbf{v}^L(j) - c_N\mathbf{v}^N(j), \quad s = r, l, \tag{35}$$

where c_L and c_N are positive constants. Note that, in principle, the frictional forces are proportional to the length of the body segment, i.e., the distance $|\mathbf{x}_s(j+1) - \mathbf{x}_s(j)|$. For the sake of simplicity, we assumed an average of the periodically varying segment length.

The physical reason for Eq. 35 is the following: the body is lying in a groove on the agar surface (see section titled Environment). If the elements of the body move perpendicularly to the local body axis ("transversal slipping"), they must either leave or deform the groove. If, on the other hand, each body element moves tangentially to the local body axis ("longitudinal slipping"), all elements (with exception of the first in the direction of movement) stay in the groove. We assume that the force needed to leave or deform the groove is greater than the force needed to slither tangentially in it. This is expressed by Eq. 35, if $c_N \gg c_L$. We chose $c_N = 10{,}000\, c_L$. We also did calculations with smaller and larger ratios c_N/c_L, with essentially the same results as the ones which will be presented below.

There is evidence that *C. elegans* amplifies the effect of the high ratio c_N/c_L by the anatomical structure of its cuticle. The evidence consists in the longitudinal ridges (alae) which run along the body of *C. elegans* in that part of the skin which is in contact with the support (Cox et al., 1981). We suggest that the function of these ridges is

to augment the ratio of the coefficients of friction for longitudinal and transversal slipping.

TRAJECTORY CONTROL

Let us assume that the worm's body is initially in a sinusoidal shape and that the neural system generates muscle excitation patterns which are suitable to propel the body either forwards or backwards. If only the forces considered until now are taken into account, the first segment of the body (in the direction of motion) will move along the tangent to the first segment of the trajectory. When the motion continues, this tangent will not change if it is determined by Eqs. 30–33. Because each element of the body follows the preceding one, one might expect that eventually the whole body will be lying along a straight line. Because only curved parts of the body contribute to the propelling force (see, e.g., Gray, 1953; Erdös and Niebur, 1990), it will come to a stand still. This is indeed observed in a computer simulation, when Eqs. 32 and 33 are used to describe the motion of the head and tail.

The worm solves this problem in such a way that its head does not follow the tangent of its own trajectory, but wiggles left and right as it moves forwards. This generates the curvature of the body which is necessary for its propulsion. The movements of the head of *C. elegans* are performed by a set of muscles which receive a more detailed innervation than the somatic musculature in the other parts of the body. We do not attempt to explain in detail the function of the neurons which control the movement of the head. Instead, we suppose that they are capable of controlling the head muscles in such a manner that the nematode's head advances along a sinusoidal trajectory. Our assumption of a sine curve for the wavelike trajectory is not essential, but simplifies the calculations.

Hence, the position of a point was calculated, towards which the head would turn during the next phase of motion to assure a sinusoidal track. Because the body glides much more easily along the groove than perpendicular to it (see previous section), it suffices for the head muscles to direct the head towards this point. The rest of the body will then follow the first segment, i.e., the head.

In the mathematical simulation of the motion, this procedure was implemented by controlling the direction of the tangent for the head segment. (Note that no external force was applied to the head segment. The contrary would be unrealistic and could be misleading in a simulation, since it might lead to a movement of the worm without the use of its muscles.) Let us define a quantity d as

$$d = 2x_l(N) + 2x_r(N) - x_l(N-1) - x_r(N-1). \quad (36)$$

In analogy to Eq. 2 and using the same constants A and k as there, we define a quantity u by

$$u = A \cos(kd). \quad (37)$$

We can now determine the point $\mathbf{X}$ to which the head must be directed:

$$\mathbf{X} = \begin{pmatrix} X \\ Y \end{pmatrix}, \quad (38)$$

with

$$X = d \pm \frac{u}{\sqrt{1+u^2}} \quad (39)$$

and

$$Y = A \sin(kd) \pm \frac{-u}{\sqrt{1+u^2}} \quad (40)$$

Here, the upper or lower sign applies for $s = r$ or $s = l$, respectively. These definitions enable us to write down the formula which replaces Eq. 34 and has been used for the head

$$\mathbf{v}_s^L(N) = [\mathbf{v}_s(N) \cdot \mathbf{n}_s]\mathbf{n}_s. \quad (41)$$

where $\mathbf{n}_s$ is a unit vector in the direction of $\mathbf{X} - \mathbf{x}_s(N)$. Similar equations were developed for the tail segment ($i = 1$).

EQUATIONS OF MOTION

According to Newton's second law, the inertial forces (i.e., mass times acceleration) acting on a body equal the sum of all other forces acting on the body. These other forces are the interior forces (caused by pressure, cuticle elasticity, and muscles), and the forces of friction resulting from the interaction with the environment. As explained in the section titled Forces exerted by the environment, inertial forces can be neglected.

Let $\mathbf{F}_r(j)$ be the sum of the interior forces which act on the point $\mathbf{x}_r$, on the right side of the body, i.e., $F_r(j)$ is the sum of the forces resulting from the interior pressure, the muscles, and the elastic cuticle:

$$\mathbf{F}_r(j) = \mathbf{F}_r^{(p)}(j) + \mathbf{F}_r^{(m)}(j, j-1) + \mathbf{F}_r^{(m)}(j, j+1) + \mathbf{F}_r^{(e)}(j) + \mathbf{F}_r^{(e)}(j, j-1) + \mathbf{F}_r^{(e)}(j, j+1). \quad (42)$$

The forces appearing on the right-hand side of Eq. 42 were introduced in earlier sections. This equation is

valid, as it stands, for interior segments. The corresponding expressions for the ends, i.e., for $j = 1$ and $j = N$, are analogous.

Let $\mathbf{F}_r^{(L)}(j)$ be the component of $\mathbf{F}_r(j)$ which is parallel to $\mathbf{v}_r^{(L)}(j)$, i.e., the longitudinal force, and let $\mathbf{F}_r^{(N)}(j)$ be the component of $\mathbf{F}_r(j)$ which is parallel to $\mathbf{v}_r^{(N)}(j)$, i.e., a force transverse to the body axis. From Newton's second law, which can be stated as

$$\mathbf{F}_r(j) + \mathbf{F}_r^{(f)}(j) = 0, \quad \text{for all } j,$$

where $\mathbf{F}_r^{(f)}(j)$ is the frictional force (35), and from Eq. 34, we obtain,

$$\frac{d}{dt}\mathbf{x}_r^{(L)}(j) = \frac{1}{c_L}\mathbf{F}_r^{(L)}(j), \tag{43}$$

$$\frac{d}{dt}\mathbf{x}_r^{(N)}(j) = \frac{1}{c_N}\mathbf{F}_r^{(N)}(j). \tag{44}$$

The vectors $\mathbf{x}_r^L(j)$ and $\mathbf{x}_r^N(j)$ are defined by these equations, i.e., by the time integral of the longitudinal and normal velocities introduced in (31 and 32). If the initial conditions are chosen correctly, we will have

$$\mathbf{x}_r(j) = \mathbf{x}_r^L(j) + \mathbf{x}_r^N(j),$$

at all times. For the points on the left of the body we obtain

$$\frac{d}{dt}\mathbf{x}_l^{(L)}(j) = \frac{1}{c_L}\mathbf{F}_l^{(L)}(j), \tag{45}$$

$$\frac{d}{dt}\mathbf{x}_l^{(N)}(j) = \frac{1}{c_N}\mathbf{F}_l^{(N)}(j). \tag{46}$$

It is evident that the forces $\mathbf{F}_r(j)$ and $\mathbf{F}_l(j)$ and the coordinates $\mathbf{x}_r(j)$ and $\mathbf{x}_l(j)$ are functions of time. We do not write the argument t.

The Eqs. 43–46 form a system of $4N$ ordinary differential equations. No analytical solution of this system is known, because the forces $\mathbf{F}_r(j)$ and $\mathbf{F}_l(j)$ and their components are nonlinear functions of the set of coordinates. The simulation of the movement of the nematode is obtained by solving this system of equations numerically, with the initial conditions given in Eqs. 3–5.

Note, that it follows from the definition of the forces introduced, that the sum of all interior forces vanishes. It is easily verified that

$$\sum_{j=1}^{N} [\mathbf{F}_r^{(z)}(j) + \mathbf{F}_l^{(z)}(j)] = 0, \quad z = p, e, \tag{47}$$

$$\sum_{j=1}^{N-1} [\mathbf{F}_s^{(z)}(j, j+1) + \mathbf{F}_s^{(z)}(j+1, j)] = 0, \quad z = e, m; s = r, l. \tag{48}$$

From these equations, it follows

$$\sum_{j=1}^{N} [\mathbf{F}_r(j) + \mathbf{F}_l(j)] = 0. \tag{49}$$

The fulfillment of these conditions was continuously monitored during the calculation to assure the accuracy of the results.

COMPUTER SIMULATION OF UNDULATORY LOCOMOTION

In the first part of this section, we will give the numerical parameters used for the computer simulation. Subsequently, we will describe the computer model used for simulating the stretch receptor control, and present the results of the computer simulation.

Mathematically, the computer simulation consists of the numerical solution of Eqs. 43–46 with the initial conditions given in Eqs. 3–5. The solution is obtained by the use of the Backward Differentiation Formula (see, e.g., Press et al., 1986). The computing algorithm used variable time steps: when the results converged well, automatically longer time steps were used; in case of bad convergence the time steps were diminished.

The equation of motion is a stiff equation in the range of parameters which interests us. We solved it using the backward differentiation method in the form of an algorithm written by us, as well as by means of a commercially available scientific subroutine package (NAG, 1987). The results were practically identical, but the NAG routine proved to be considerably faster and was used for all results presented in this manuscript. The nonlinear equations arising from the backward differentiation method were solved using a modified Newton method. On entrance, the routine performs a local error Petzold test. The tolerance was chosen such that the absolute error does not exceed 10^{-7} and the relative error does not exceed 10^{-4} for any of the $4N$ equations (using the maximum norm).

Furthermore, different tests were carried out during the integration of the differential equations, such as a check on the accuracy to which the Eqs. 47–49 were satisfied. Any result which led to a violation of relative order 10^{-5} or more of any of these equations was rejected and recalculated from the previous time step with higher requirements on the tolerance. This happened rarely with our own backward differentiation routine and never with the NAG routine.

The calculation of the data shown in Fig. 4 required several hours of CPU time of a Cray-2 supercomputer. The details of the numerical calculations may be found

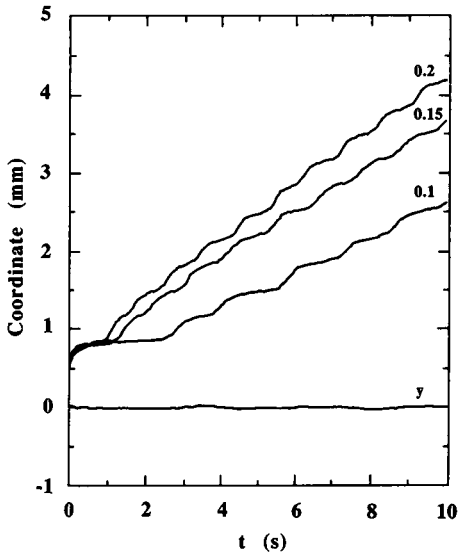

FIGURE 4 Position of the center-of-mass of the simulated worm as a function of time. The three ascending curves show the x-coordinate of the center-of-mass for $g = 0.1$, 0.15, and 0.2, respectively; see Eq. 54. The lowest curve, marked by y, represents the y-coordinate of the center-of-mass for $g = 0.1$. Like the corresponding curves for $g = 0.15$ and $g = 0.2$ (not shown), the curve y is very close to zero, which shows that the worm moves almost exactly parallel to the x-axis. The amplitude and the wavelength of the body wave are $A = 12 \cdot 10^{-5}$ m and $k = 12\pi \cdot 10^{-5}$ m, respectively. The frequency of the waves is 0.43/s ($g = 0.1$), 0.33/s ($g = 0.15$), and 0.25/s ($g = 0.2$).

in (Niebur, 1988). One reason for the length of calculations is the fact that if one segment of the body contracts, the pressure changes in all segments, so that there is a link between all segments and not only between adjacent ones.

Initialization and numerical solution procedure

Table 2 shows the numerical values which have been used for the computer simulation of a creeping *C. elegans*. The radius r_c and the length l_c of the cylinder, which approximates the body of the nematode, are experimentally known quantities. The other parameters in Table 2 are not known from experiment and must be chosen on the basis of plausibility arguments.

TABLE 2 **Parameters used for the simulations**

$l_c[m]$	$r_c[m]$	$p(0)$[Pa]	$c_L[kg/s]$	$c_N[kg/s]$	N
10^{-3}	$4 \cdot 10^{-5}$	10^4	$1.6 \cdot 10^{-3}/N$	$16/N$	20

l_c: equilibrium body length; r_c: equilibrium body radius; $p(0)$: equilibrium pressure of body liquid; c_L, c_N: longitudinal and transversal friction coefficients; N: number of model body segments.

The pressure $p(0)$ of the intestinal liquid is chosen as 10^4 Pa, which is the mean value observed in *Ascaris l.* (Lee and Atkinson, 1976). The tangential friction coefficient c_L has been chosen such that the simulated worm moves with a velocity of the order of 1 mm/s, which is the typical velocity of a creeping *C. elegans*. The perpendicular friction coefficient c_N is supposed to be much greater than c_L; we have chosen $c_N = 10{,}000\ c_L$. The simulation shows that the simulated worm creeps practically without lateral slipping for this ratio of c_N to c_L. The number of segments has been chosen as $N = 20$ for all calculations whose results are shown below. We did some simulations with lower and higher ratios of c_N to c_L, and obtained essentially the same results.

Calculations were also done with $N = 50$ segments: the results are not included because they show no significant improvement upon those for 20 segments.

Calculations with 50 segments evidently require much more computer time than work with 20 segments. In the test runs made with 50 segments, the character of the motion was the same as that obtained with 20 segments. The motion was smoother, in that the variation of the speed manifested by the wiggles in the curves showing the center-of-mass coordinate vs. time (Fig. 4) was smaller.

The cost of computation is roughly proportional to the cube of the number of equations. Therefore we felt that it was not justified to repeat all our computations using a finer segmentation of the body.

For $t = 0$, the shape of the simulated worm is given by Eq. 3 and shown in Fig. 1. This shape is chosen as a convenient starting point for the simulation. The development of this initial state as a function of time is determined by Eqs. 43–46.

A trial simulation was first done under the assumption that the body muscles are not excited, i.e., $f_r^{(m)}(j) = f_l^{(m)}(j) = 0$ for all j. The body did attain a resting state, with vanishing left-hand sides in Eqs. 43–46. (In fact, the state attained is metastable, because for $c_L < \infty$ and $c_N < \infty$, the body is in a stable state only if it is straight. This can be seen, for example, if c_L is chosen as in Table 2, and $c_N = 2c_L$. In this case the worm's body is nearly straight after ~10 s of simulated time.) It did not move either forwards or backwards as can be seen in Fig. 5, which shows the body's position after $t = 2$ s.

Muscle control by stretch receptors

Muscle forces must be introduced to obtain active motion. In the following, we will present muscle excita-

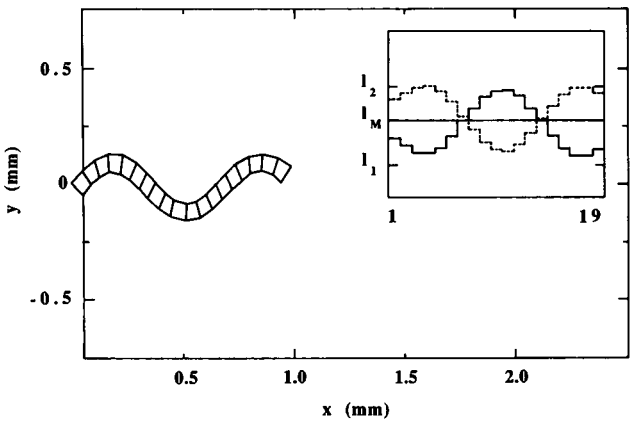

FIGURE 5 Computer simulation with vanishing muscle forces. The figure shows the shape of the worm after $t = 2$s, the shape at $t = 0$ being described in Fig. 1. The resting state has been attained and the worm has not moved forward. Its position is the same as at $t = 0$ (Fig. 1) (cf Section titled Initialization and numerical solution procedure). For the meaning of the inset, see the caption of Fig. 1.

tion patterns which lead to a sinusoidal movement of the worm.

We will now discuss local control, i.e., the control of individual muscles. If the worm is to move forward, the forces exerted by the nematode on its environment must be such that the reaction forces provide a net forward thrust to the body. Suitable muscle excitation patterns have been identified for the analogous problem in snakes (Gray, 1953). The existence of a rigid backbone facilitates the analysis of the forces in snakes, because the forces acting on each vertebrum can be analyzed separately. In nematodes, the problem is more complicated, because all body parts interact with each other via pressure changes in the pseudocoelom. Therefore, we resorted to computer simulations to find excitation patterns that lead to forward movement.

There are several solutions to the problem (Niebur, 1988). We are here concerned only with the one which can be generated by stretch receptors in *C. elegans*. These stretch receptors, which have been postulated first by R. L. Russell (personal communication) on morphological grounds but have not been unequivocally identified yet, are situated approximately a fifth of the body length behind (with respect to the motion of the body) the muscles they control. In the following, we will formalize the control scheme and we will show in the next section that this scheme is suitable for propelling the nematode body.

It is shown in (Niebur, 1988) how the nematode nervous system can exert a global control over the somatic musculature, i.e., how the worm can change its direction of motion (forwards or backwards) and stop.

We use again the subscript s to designate the side of the body (left, l, or right, r), and define a variable Δ which is 1 if the body moves in the positive x direction and is -1 if the body moves in the opposite direction. The distance between the sensitive part of a receptor and the muscle it controls is assumed to be $l_c/5$.

Let us define the mean length l_M of the $N - 1$ segments,

$$l_M = \frac{1}{2N} \cdot \left\{ \sum_{j=1}^{N-1} |\mathbf{x}_r(j+1) - \mathbf{x}_r(j)| + \sum_{j=1}^{N-1} |\mathbf{x}_l(j+1) - \mathbf{x}_l(j)| \right\}. \quad (50)$$

Consider the following conditions on the length of segment j:

$$\left| \mathbf{x}_s\left(j + 1 - \Delta\frac{N}{5}\right) - \mathbf{x}_s\left(j - \Delta\frac{N}{5}\right) \right| > l_M, \quad s = r, l; \quad (51)$$

$$|\mathbf{x}_s(j+1) - \mathbf{x}_s(j)| > l_M, \quad s = r, l; \quad (52)$$

and

$$j \in \begin{cases} \left\{2 + \frac{N}{5}, \cdots; N - 2\right\} & \text{if } \Delta = 1; \\ \left\{2; \cdots; N - \frac{N}{5} - 1\right\} & \text{if } \Delta = -1. \end{cases} \quad (53)$$

Condition 51 is the model of an excitatory receptor within a distance of $l_c/5$ from the muscle to be controlled by it. Condition 52 restricts the muscle excitation to those segments which are compressed to a length which is greater than the average length of a segment. The condition 53 defines the values of j for which conditions 51 and 52 hold.

The muscle excitation pattern (see Eq. 51) is defined by

$$f_s^{(m)}(j) = \begin{cases} g & \text{if the conditions in Eqs. 51–53 are fulfilled} \\ 0 & \text{otherwise.} \end{cases} \quad (54)$$

In this equation, g is a dimensionless number which is usually chosen as a fraction of unity.

It would be more realistic to assume that the muscle excitation is a continuous process and not abrupt as described by Eq. 54, but this would complicate the model.

NEMATODE LOCOMOTION

An example of a muscle excitation pattern generated by stretch receptor control is shown in Fig. 6. The pattern is similar to that which is used by a creeping snake (cf Gray, 1953). The calculation shows that the simulated

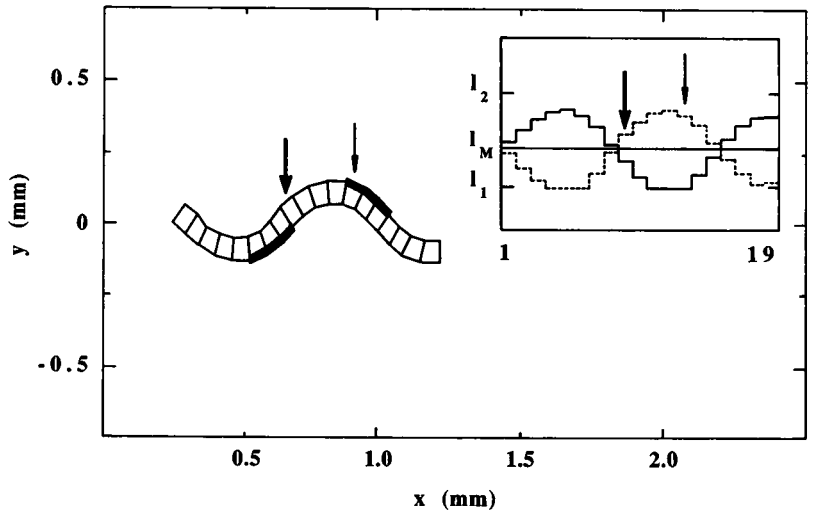

FIGURE 6 Muscle control by stretch receptors. To illustrate the stretch receptor control, one segment (the ninth) is marked by a thick arrow, both in the figure and in the inset. It is seen that the length of this segment on the right side of the body is greater than l_M (*dotted line in inset*), and it is smaller than l_M on the left side of the body (*full line in inset*). Following Eq. 54 and using $\Delta = 1$, the muscles of the right side of segment 13 are excited, but not those of the left side. In the figure, excited muscles are represented by thick lines. Segment 13 is marked by a thin arrow, both in the figure and in the inset. Note that the stretch receptor is located behind the muscle it controls because the worm moves in $(+x)$ direction.

worm is able to move in its environment, from which it follows that this pattern is suitable for propelling the body. This proves that nematodes can control their undulatory locomotion by stretch receptors.

Fig. 7 shows three successive phases of the motion. Fig. 4 represents the coordinates of the center-of-mass of the simulated worm vs. time. In each of these curves, the gradient, which corresponds to the velocity of the simulated worm, varies with time. This is due to the acceleration of the body each time the head passes a wave crest, because at that time a segment whose muscles were not contracted previously, contracts, and contributes to the propulsive force. This variation of the velocity of the center of mass, which is not observed in a moving nematode, is probably caused by the subdivision of the body into segments. It is less pronounced if $N = 50$ rather than $N = 20$ is chosen (data not shown).

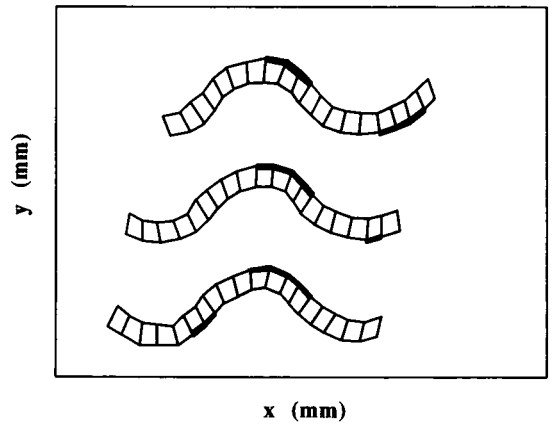

FIGURE 7 Three successive phases of the motion of the simulated worm as it is shown on the computer screen. The position of the worm is shown at $t = 0.8$ s (*bottom*), $t = 2.3$ s (*middle*), and $t = 2.8$ s (*top*). To avoid partial superposition, the lower and upper drawings have been displaced from the middle one in the y direction. The worm moves in the $(+x)$ direction.

The three curves shown in Fig. 8 are obtained using three different values for g, i.e., the amplitude of the muscle force, which has been defined in Eq. 54. This parameter is identical for all segments and can thus be varied globally. It follows from the observation that the mean slopes of these curves are different, that the worm can vary its velocity by varying this global parameter. This can be accomplished in the nematode neural system by changing the excitation of the interneurons presynaptic to the motor neurons.

Fig. 8 shows that our model also allows for a change in the direction of motion. This is achieved by deactivating the neural circuitry which is responsible for forward motion, and activating the circuitry which is responsible for backward motion, or vice-versa. In the calculation shown, this switch is simulated by changing the sign of Δ in Eq. 53, when the end of the worm has reached a predefined value of x. As a result, the simulated worm creeps back on its own track. This mirrors the behavior of a real worm, when it changes its direction of motion.

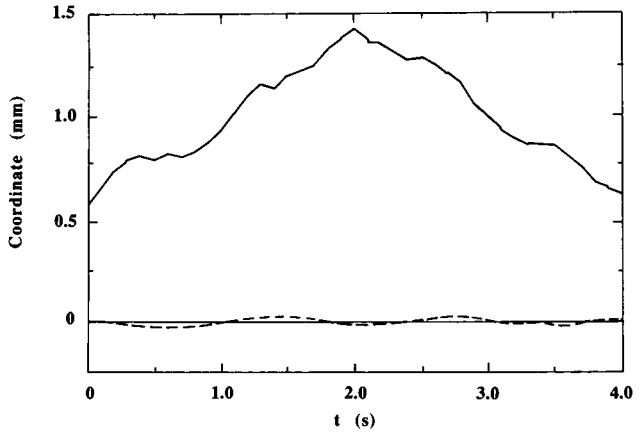

FIGURE 8 Changing the sign of Δ leads to the change of direction of the movement. At $t = 0$, the motion is started with $\Delta = 1$, and $g = 0.2$. As soon as x_1 exceeds the value 1, which is the case at $\sim t = 2$s, Δ takes the value (-1) and the worm changes the direction of its motion. The full line shows the x-coordinate of the worm's center-of-mass, and the dashed line its y-coordinate.

CONCLUSION

We have studied the undulatory motion of animals with hydrostatic skeletons, in particular that of the nematode *C. elegans*. We have identified the most important forces which act on a creeping nematode, and established a mathematical model of these forces. This makes it possible to simulate with a computer the creeping of the nematode. It is known from experiments that *C. elegans* has two nearly distinct neural circuits, one for forward and another for backward movement. We assume (*a*) that the nerve ring activates one or the other of these circuits, and that the level of activation determines the velocity of the worm, and (*b*) that the detailed muscle excitation patterns are not determined globally by the nerve ring, but locally by stretch receptors in the motor neurons which are presynaptic to the somatic muscles. The computer simulation shows that these excitation patterns can be produced by the action of stretch receptors, for which anatomical evidence has been observed by other work.

Some nematodes can vary the wavelength of their motion over a range of at least a factor of four depending on the impedance of their surroundings. We have not observed such a variation in *C. elegans* moving on dry or wet agar or inside the agar. We are aware of the fact that the wavelength of *C. elegans* increases appreciably when the worm is swimming in water. This change of body shape is always correlated with a change in the physics of the environment. It is unknown whether the changed body form is a consequence of a changed motor pattern, which might lead to more efficient propulsion in the respective environment, or whether it is due to a (passive) deformation of the body. This passive deformation may be due to the fact that in different environments, different external forces act on the body even though the muscles are controlled by the same motor control program. The two environments, which are at the extremes of the spectrum a nematode might encounter, are one in which the worm creeps without slipping (and which is treated by our model) and one in which the animal is swimming in a liquid of low viscosity, like water. As we have shown previously, it is not easy to treat the case of a swimming worm and to decide whether the motor control pattern used for creeping yields the observed body shape when the worm is immersed in water. Our hypothesis is that this is the case. Evidence in support of this hypothesis is provided by the fact that nematodes always seem to have the same wavelength in a given physical environment. If the animals were able to change their motor pattern (and thus their body shape) "at will," one might expect the nematode to change its motor pattern also in response to other factors than the mechanical impedance of the surroundings, such as sensory stimuli. To the best of our knowledge, this has never been observed.

In the absence of either experimental evidence or more detailed model calculations (taking into account inertial and viscous forces), our model remains a hypothesis to be verified or refuted by further experiments.

A videotape has been produced by filming the actual motion of a *C. elegans* and filming the graphical representation on a computer screen of the simulated results. The simulation reproduces well the actual motion. Copies of the videotape may be obtained from the authors.

APPENDIX

Elsewhere we have developed a mathematical model for electrotonic neural networks and applied it to the nervous system of nematodes (Erdös and Niebur, 1990, Niebur and Erdös, 1988*a*, *b*, 1991). The following results are relevant for the present work: *Caenorhabditis elegans* (of length ~ 1 mm) is the only animal of which the complete neural circuitry is known at the submicroscopical level. This anatomical knowledge is complemented by functional insight from electrophysiological experiments in the related nematode *Ascaris lumbricoides* (length $\sim 1{,}000$ mm), which show that *Ascaris* motor neurons transmit signals electronically and not with unattenuated spikes.

We formulated partial differential equations for the intracellular voltage of the neural processes, and solved them numerically. One of the results is that the nerve ring (central nervous system) in the head of *C. elegans* is capable of producing signals which, even though attenuated electrotonically, are sufficiently strong to control all motor neurons. Furthermore, we found that in *Ascaris l.* the velocity of the travelling neural excitation is close to the experimentally observed velocity of travel of muscular waves. In *C. elegans* however, all observed muscular waves propagate at least ten times slower than the calculated

neural excitation waves. Therefore, the excitation wave cannot synchronously control the muscular wave. From the observation of neural processes of appropriate length, we suggest control by stretch receptors, which transmit signals to muscles which are ¼ body wavelength anterior or posterior to the activated stretch receptors.

A prerequisite for this mechanism is the presence of two distinct neural circuits for forward and backward motion: these circuits have been experimentally identified.

This work was supported by the Swiss National Science Foundation through grants 2000-5.295 and 20-28846.90.

Received for publication 15 August 1989 and in final form 16 July 1991.

REFERENCES

Bird, F. B. 1971. The Structure of Nematodes. Academic Press, New York.

Brenner, S. 1974. The genetics of *Caenorhabditis elegans. Genetics.* 77:71–94.

Brokaw, C. J. 1985. Computer simulation of flagellar movement VI: simple curvature-controlled models are incompletely specified. *Biophys. J.* 48:633–642.

Cox, G. N., M. Kusch, and R. S. Edgar. 1981. Cuticle of *C. elegans:* its isolation and partial characterisation. *J. Cell. Biol.* 90:7–17.

Crofton, H. D. 1971. Form,. function and behavior. *In* Plant parasitic Nematodes. B. M. Zuckermann, W. F. Mai, and R. A. Rohde, editors. Academic Press, New York. 83–113.

Edgar, R. S., G. N. Cox, M. Kusch, and J. C. Politz. 1982. The cuticle of *C. elegans. J. Nematol.* 14:248–258.

Erdös, P., and E. Niebur. 1990. The Neural basis of the locomotion of nematodes. *In* Lecture Notes in Physics. Vol. 368. L. Garrido, editor. Springer Verlag, Berlin. 253–267.

Fredericksen, D. W., and R. D. Specian. 1981. The value of cuticular fine structure in identification of juvenile anisakine nematodes. *J. Parasitol.* 67:647–655.

Gray, J. 1953. Undulatory propulsion. *Q. J. Microsc. Sci.* 94:551–578.

Gray, J., and H. W. Lissmann. 1964. The locomotion of nematodes. *J. Exp. Biol.* 41:135–154.

Harris, J. E., and H. D. Crofton. 1957. Structure and function in the nematodes: internal pressure and cuticular structure in *Ascaris. J. Exp. Biol.* 34:116–130.

Johnson, C. D., and A. O. W. Stretton. 1980. Neural control of behavior in nematodes: anatomy, electrophysiology, and biochemistry. *In* Nematodes as Biological Models. Vol. 1. B. M. Zuckermann, editor. Academic Press, New York, 159–195.

Lee, D. L., and H. J. Atkinson. 1976. Physiology of Nematodes. The Macmillan Press Ltd., London.

Morseth, D. J., and E. J. Soulsby. 1969. Fine structure of leukocytes adhering to the cuticle of *Ascaris suum* larvae. *J. Parasitol.* 55:22–31.

Nachtigall, W. 1983. The biophysics of locomotion in water. *In* Biophysics. W. Hoppe, W. Lohmann, H. Markl, and H. Ziegler, editors. Springer-Verlag, Berlin.

NAG 1987. The NAG Fortran Library Manual-Mark 12. The Numerical Algorithms Group Ltd., Oxford, UK.

Niebur, E. 1988. Théorie du système locomoteur et neuronal des Nématodes. PhD thesis. University of Lausanne, Switzerland.

Niebur, E., and P. Erdös. 1991. Control of the Undulatory Motion of Vermiform Bodies. In Progress in Robotics and Intelligent Systems. G. Zobrist, editor. Ablex Publishing Company, Norwood, N. J. In press.

Niebur, E., and P. Erdös. 1988*a*. Computer simulation of the motor-neural system of a simple invertebrate. *Neural Networks.* (Supplement) 1:350–.

Niebur, E., and P. Erdös. 1988*b*. Computer simulation of networks of electrotonic neurons. *In* Computer Simulation in Brain Science. R. M. Cotterill, editor. Cambridge University Press, Cambridge. 148–163.

Press, W. H., B. F. Flannery, S. A. Teukolsky, and W. T. Vetterling. 1986. Numerical Recipes. Cambridge University Press, Cambridge.

Rikmenspoel, R. 1978. The equation of motion for sperm flagella. *Biophys. J.* 23:177–206.

Stretton, A. O. W. 1976. Anatomy and development of the somatic musculature of the nematode *Ascaris. J. Exp. Biol.* 64:773–788.

Thust, R. 1966. Elektronenmikroskopische Untersuchungen über den Bau des larvalen Integumentes und zur Häutungsmorphologie von *Ascaris lumbricoides. Zool. Anz.* 177:411–417.

Toida, N., H. Kuriyama, N. Tashiro, and Y. Ito. 1975. Obliquely striated muscle. *Physiol. Rev.* 55:700–756.

Wallace, H. R. 1969. Wave formation by infective larvae of the plant parasitic nematode *Meloidogyne javanica. Nematologica.* 15:67–75.

Weisblat, D. A., and R. L. Russell. 1976. Propagation of electrical activity in the nerve cord and muscle syncyticum of the nematode *Ascaris lumbricoides. J. Comp. Physiol.* 107:293–307.

White, J. G., E. Southgate, J. N. Thomson, and S. Brenner. 1986. The structure of the nervous system of the nematode *Caenorhabditis elegans. Phil. Trans. R. Soc. Lond. B. Biol. Sci.* 314:1.